

The catalytic role of beta effect in barotropization processes

A. VENAILLE¹†, G. K. VALLIS¹
AND S. M. GRIFFIES¹

¹ NOAA, GFDL, AOS Program, Princeton University, NJ 08540, USA.

(Received March 15, 2019)

The vertical structure of freely evolving, continuously stratified, quasi-geostrophic flow is investigated. We predict the final state organization, and in particular its vertical structure, using statistical mechanics and these predictions are tested against numerical simulations. The key role played by conservation laws in each layer, including the fine-grained enstrophy, is discussed. In general, the conservation laws, and in particular that enstrophy is conserved layer-wise, prevent complete barotropization, i.e., the tendency to reach the gravest vertical mode. The peculiar role of the β -effect, i.e. of the existence of planetary vorticity gradients, is discussed. In particular, it is shown that increasing β increases the tendency toward barotropization through turbulent stirring. The effectiveness of barotropisation may be partly parameterized using the Rhines scale $2\pi E_0^{1/4}/\beta^{1/2}$. As this parameter decreases (beta increases) then barotropization can progress further, because the beta term provides enstrophy to each layer. However, if the beta effect is too large then the statistical mechanical predictions fail and wave dynamics prevent complete barotropization.

1. Introduction

The vertical structure of eddying flow in the oceanic mesoscale is a fundamental problem in geophysical fluid dynamics, one that has been reinvigorated by the need to interpret altimetric observation of surface velocity fields (Scott & Wang 2005; Lapeyre 2009). Energy cascades and self-organization processes are fairly well understood and characterized in two-dimensional turbulence, but how these results generalize to rotating, continuously stratified flows is still an open question. We ask in this paper what is the final organization of a freely evolving inviscid quasi-geostrophic flow with continuous stratification. In particular, we examine what are the precise conditions for the oft-cited barotropization process to occur. Barotropization refers to the tendency of a quasi-geostrophic flow to reach the gravest vertical mode (Charney 1971; Rhines 1977). Because the gravest vertical mode is the barotropic one, i.e. a depth independent flow, “barotropization” means a tendency toward the formation of depth independent flows. We study in particular the key role played by the beta effect (the existence of planetary vorticity gradients) in such barotropization processes. It has been previously noticed that the presence of these large scale planetary vorticity gradients favors barotropic process, see e.g. Smith & Vallis (2001), but this phenomenon remains to our knowledge unexplored and unexplained.

Continuously stratified quasi-geostrophic flows take place in three dimensions, but their dynamics are quasi-two-dimensional because the non-divergent advecting velocity field has only horizontal components. The dynamics admits similar conservation laws as the two-dimensional Euler equations, including among others the total energy and the enstrophy of each layer. These conservations laws imply an inverse energy cascade toward large scales, and weak energy dissipation in presence of weak viscosity (Kraichnan & Montgomery 1980). This situation contrasts

† Present address: Laboratoire de Physique ENS-Lyon., 16 allée d’Italie 69007 Lyon, France

with three dimensional turbulence where the energy cascades forward toward small scales, giving rise to finite energy dissipation no matter how weak the viscosity.

Just as for two-dimensional Euler flows, inviscid, freely evolving continuously stratified quasi-geostrophic flows are disordered and an unstable initial condition rapidly evolves into a strongly disordered fine-grained flow with filaments being stretched, folded, and consequently cascading toward smaller and smaller scales. However, the inverse energy cascade leads to the formation of robust, large scale coherent structures filling the domain in which the flow takes place, contrasting strongly with the analogous three dimensional flow with its energy transfer to small scales.

The aim of this paper is to provide a prediction for the vertical structure of the large scale flow organization resulting from inviscid, freely evolving continuously stratified quasi-geostrophic dynamics using a statistical approach. The goal of the statistical mechanics approach is to drastically reduce the complexity of the problem of determining the large scale flow organization to the study of a few key parameters given by the dynamical invariants, as for instance the total energy and the fine-grained enstrophy in each layer. Such a theory has been independently proposed by Robert (1990); Robert & Sommeria (1991) and Miller (1990), and henceforth will be referred to as MRS theory. It is an equilibrium theory, developed in the case without forcing and dissipation. Our contribution will be to apply this theory to the explicit computation of a class of equilibrium states of the stratified quasi-geostrophic equations in the presence of a planetary vorticity gradient.

A crucial ingredient of the theory comes from the constraints given by dynamical invariants. In the present paper, we will focus, as a first step, on the role played by the energy and the enstrophy constraints. The phenomenology of two-dimensional and geostrophic turbulence is often explained by considering these constraints only, see e.g. Kraichnan & Montgomery (1980); Salmon (1998). Higher invariants must be taken into account in order to describe relevant geophysical turbulent coherent structures, such as Jovian vortices (Bouchet & Sommeria 2002) or oceanic rings and jets (Venaille & Bouchet 2011). There have been few previous studies of statistical equilibria of the continuously stratified quasigeostrophic dynamics. Merryfield (1998) obtained and discussed a class of solutions in the framework of energy-enstrophy statistical theory. The solutions obtained were critical points of the theory, but the actual entropy maxima were not selected. The present paper builds upon these results to show i) that these energy-enstrophy states are a particular class of MRS equilibria ii) that it is possible to relate each critical point to the energy and fine-grained enstrophy constraint iii) that it is possible to compute explicitly the actual entropy maximum in different limit cases.

Schechter (2003) provided a direct comparison between numerical simulations and numerical computation of MRS statistical equilibria, focusing on the particular case of initial conditions given by a random field statistically homogeneous in space, as in McWilliams *et al.* (1994). We will outline in this paper the important consequence of the conservation of enstrophy at each depth. This important role played by the enstrophy constraint allows us to discuss how the beta effect can favor barotropization. For a given initial streamfunction field, the beta effect modifies the initial distribution of potential vorticity, and therefore modifies the vertical profile of fine-grained enstrophy. More precisely, increasing the beta effect tends to increase the depth independent part of the fine-grained enstrophy profile. We will show that statistical equilibria associated with depth independent fine-grained enstrophy profile are barotropic, which means that increasing the beta favors barotropization, according to statistical mechanics predictions.

The paper is organized as follows: the continuously stratified quasi-geostrophic equations are introduced on section 2. The MRS equilibrium statistical mechanics theory of such systems is presented in section 3. Here it is shown that the class of MRS statistical equilibria characterized by a linear relation between potential vorticity and streamfunction are solutions of a minimum enstrophy problem, which is solved in various limit cases, first without beta effect and then with beta effect. The theory predicts an increase of barotropization with increasing value of beta,

which is tested against numerical simulations in section 4. A summary of the main results and a discussion of their application to the ocean is given section 5.

2. Continuously stratified quasi-geostrophic model

2.1. Equations of motion

We consider an initial value problem for a freely evolving, unforced, undissipated, quasi-geostrophic flow with continuous stratification $N(z)$ (see e.g., Vallis (2006), section 5.4):

$$\partial_t q + J(\psi, q) = 0, \quad (2.1)$$

$$q = \Delta\psi + \frac{\partial}{\partial z} \left(\frac{f_0^2}{N^2} \frac{\partial}{\partial z} \psi \right) + \beta y, \quad (2.2)$$

with $J(\psi, q) = \partial_x \psi \partial_y q - \partial_y \psi \partial_x q$, and $f = f_0 + \beta y$ is the Coriolis parameter with the β -plane approximation. Neglecting buoyancy and topography variations, the boundary condition at the bottom ($z = -H$, where H is a constant) is given by

$$\partial_z \psi|_{z=-H} = 0. \quad (2.3)$$

The boundary condition at the surface (defined as $z = 0$, using the rigid lid approximation), is given by the advection of buoyancy

$$\partial_t b_s + J(\psi, b_s) = 0, \quad \frac{f_0^2}{N^2} \partial_z \psi|_{z=0} = b_s. \quad (2.4)$$

2.2. Modal decomposition

2.2.1. Laplacian and baroclinic eigenmodes

We consider the case of a doubly periodic domain $\mathcal{D} = [-\pi, \pi] \times [-\pi, \pi]$. The Fourier modes $e_{k,l}(x, y)$ are a complete orthonormal basis of the 2D Laplacian $\Delta e_{k,l} = -K^2 e_{k,l}$ where (k, l) are the wavenumbers in each directions and $K^2 = k^2 + l^2$. In the vertical, the complete orthonormal basis of barotropic-baroclinic modes is defined by the solutions $F_m(z)$ of the Sturm-Liouville eigenvalue problem

$$\frac{\partial}{\partial z} \left(\frac{f_0^2}{N^2} \frac{\partial}{\partial z} F_m \right) = -\lambda_m^2 F_m \quad \text{with} \quad F'(0) = F'(-H) = 0, \quad (2.5)$$

where $m \geq 0$ is an integer, λ_m^2 is the eigenvalue associated with mode m , which defines the m^{th} -baroclinic Rossby radius of deformation λ_m^{-1} . The barotropic mode is the (depth independent) mode F_0 , associated with $\lambda_0 = 0$.

2.2.2. Surface quasi-geostrophic (SQG) modes

In the following, it will be convenient to distinguish the interior dynamics from the surface dynamics. For a given potential vorticity field $q(x, y, z, t)$ and surface buoyancy field $b_s(x, y, t)$, the streamfunction can be written $\psi = \psi_{\text{int}} + \psi_{\text{surf}}$, where ψ_{int} is the solution of

$$\Delta\psi + \frac{\partial}{\partial z} \left(\frac{f_0^2}{N^2} \frac{\partial}{\partial z} \psi \right) = q - \beta y \quad \text{with} \quad \partial_z \psi|_{z=0} = \partial_z \psi|_{z=-H} = 0, \quad (2.6)$$

and where ψ_{surf} is the solution of

$$\Delta\psi + \frac{\partial}{\partial z} \left(\frac{f_0^2}{N^2} \frac{\partial}{\partial z} \psi \right) = 0, \quad \text{with} \quad \partial_z \psi|_{z=0} = \left(\frac{N(0)}{f_0} \right)^2 b_s, \quad \partial_z \psi|_{z=-H} = 0 \quad (2.7)$$

Each projection of ψ_{surf} on a (horizontal) Laplacian eigenmode (l, k) defines a surface quasi-geostrophic eigenmode (SQG mode hereafter). When the stratification N is constant and when $f_0/(NK) \ll H$, these SQG modes are decreasing exponential functions

$$\widehat{\psi}_{\text{surf},k,l} = A_{k,l} e^{zNK/f_0} + O\left(\frac{h_K}{H}\right), \quad (2.8)$$

where the coefficients $A_{k,l}$ are determined using the boundary condition at the surface. When the stratification is not constant, but when $f_0/N(0)K \ll H$, the SQG modes are still characterized by a decreasing exponential, with an e -folding depth $h_K = f_0/KN(0)$.

The distinction between surface and interior streamfunction is sometime useful to describe the dynamics, see e.g. Lapeyre & Klein (2006), but a shortcoming of such a decomposition is that ψ_{int} and ψ_{surf} are not orthogonal.

2.3. Delta-sheet approximation and SQG-like modes

The boundary condition (2.4) can be formally replaced by the condition of no buoyancy variation ($\partial_z \psi = 0$ at $z = 0$), provided that surface buoyancy anomalies are interpreted as a thin sheet of potential vorticity just below the rigid lid (Bretherton 1966). For this reason, and without loss of generality, we will consider that $b_s = 0$ in the remaining of this paper.

Let us now consider a case with no surface buoyancy, but with a surface intensified potential vorticity field defined as $q = q_{\text{surf}}(x, y)\Theta(z + H_1) + q_{\text{int}}(x, y, z)$, with $H_1 q_{\text{surf}} \gg H q_{\text{int}}$, $H_1 \ll H$ and Θ the Heaviside function. Using the linearity of (2.6), one can still decompose the streamfunction field into $\psi = \psi_{\text{surf}} + \psi_{\text{int}}$ where ψ_{surf} is the flow induced by the PV field $q = q_{\text{surf}}\Theta(z + H_1)$, obtained by inverting (2.2), and ψ_{int} the flow induced by q_{int} . For $z < -H_1$, the streamfunction ψ_{surf} satisfies equation (2.7), just as SQG modes. This is why we call it an SQG-like mode.

3. Equilibrium statistical mechanics of stratified quasi-geostrophic flow

In this section we briefly introduce the MRS equilibrium statistical mechanics theory, and introduce a general method to compute the MRS equilibria. This allows for explicit computation of statistical equilibria on the f -plane in subsection 3.3, and on the β -plane in subsection 3.4.

3.1. Theory

Let us consider an initial (fine-grained) PV field $q_0(x, y, z)$. The dynamics (2.1) induced by this PV field stirs the field itself, which rapidly leads to its filamentation at smaller and smaller scale, with the concomitant effect of stretching and folding. There are two (related) consequences, one in phase space, one in physical space.

In physical space, the filamentation toward small scales implies that after a sufficiently long time evolution, the PV field can be described at a macroscopic level by a probability field $\rho(x, y, z, \sigma, t)d\sigma$ to measure a given PV level between σ and $\sigma + d\sigma$ at a given point (x, y, z) . This probability distribution function (pdf hereafter) ρ is normalized locally

$$\forall x, y, z \quad \mathcal{N}[\rho] = \int_{\Sigma} d\sigma \rho = 1, \quad (3.1)$$

where the integral is performed over the range Σ of PV levels, which is prescribed by the initial condition. The field ρ is a macrostate because it is associated with a huge number of fine-grained PV fields configurations $q(x, y, z)$ (the microscopic states), in the sense that many realizations of the (microscopic, or fine-grained) PV field q leads to the same macroscopic state ρ .

The phase space is defined by all configurations of the field $q(x, y, z)$. The cornerstone of the theory is to assume that stirring allows the system to explore evenly each possible configuration of the phase space that satisfies the constraints of the dynamics, so that these configurations can

be considered as equiprobable. When this assumption fails, as in the linear regime discussed in section 4.4, the statistical theory fails.

The main idea of the theory is then to count the number of microstate configurations associated with a macrostate (the pdf field ρ), and to say that the equilibrium state is the most probable macrostate that satisfies the constraints of the dynamics, i.e. the one that is associated with the largest number of microstates satisfying the constraints. One can then show that an overwhelming number of microstates are associated with this most probable macrostate (Michel & Robert 1994). An important physical consequence is that that an observer who wants to see the actual equilibrium macrostate would neither need to perform ensemble average nor time average, but would simply have to wait a sufficiently long time.

Note that the output of the theory is the pdf field ρ , but the quantity of interest to describe the flow structure is the coarse-grained PV field defined as

$$\bar{q} = \int_{\Sigma} d\sigma \sigma \rho. \quad (3.2)$$

In practice, counting the number of microstates q associated with a macrostate ρ is a difficult task, because q is a continuous field, and it requires the use of large deviation theory. However, it can be shown that classical counting arguments do apply here, and that the most probable state ρ maximizes the usual Boltzmann mixing entropy

$$\mathcal{S} = - \int_{\mathcal{D}} dx dy \int_{-H}^0 dz \int_{\Sigma} d\sigma \rho \ln \rho, \quad (3.3)$$

see Bouchet & Corvellec (2010) and references therein for further details.

Let us now collect the constraints that ρ must satisfy, in addition to the local normalization (3.1). An infinite number of constraints are given by conservation of the global distribution of PV levels $\mathcal{P}(\sigma, z)$, which is prescribed by the initial global distribution of PV levels $P_0(\sigma, z)$:

$$\mathcal{P}(\sigma, z)[\rho] = \int_{\mathcal{D}} dx dy \rho = P_0(\sigma, z). \quad (3.4)$$

These conservation laws include the conservation of the fine grained enstrophy

$$\int_{\mathcal{D}} dx dy \int_{\Sigma} d\sigma \sigma^2 \rho = Z_0 \quad (3.5)$$

Another constraint is given by the conservation of the total energy

$$\mathcal{E} = \frac{1}{2} \int_{-H}^0 dz \int_{\mathcal{D}} dx dy \left((\nabla \psi)^2 + \frac{f_0^2}{N^2} (\partial_z \psi)^2 \right) \quad (3.6)$$

Because an overwhelming number of microstates are close to the equilibrium state ρ , the energy of the fluctuations are negligible with respect to the energy due to the coarse-grained PV field \bar{q} (Michel & Robert 1994). Integrating by parts and replacing q by \bar{q} gives the constraint $E_0 = \mathcal{E}[\rho]$, where E_0 is the energy of the initial condition, and where

$$\mathcal{E} = \frac{1}{2} \int_{-H}^0 dz \int_{\mathcal{D}} dx dy (\beta y - \bar{q}) \psi = \frac{1}{2} \int_{-H}^0 dz \int_{\mathcal{D}} dx dy \int_{\Sigma} d\sigma (\beta y - \sigma) \psi \rho. \quad (3.7)$$

Finally, the MRS theory provides a variational problem.

$$S(E_0, P_0(\sigma, z)) = \max_{\rho, \mathcal{N}[\rho]=1} \{ \mathcal{S}[\rho] \mid \mathcal{E}[\rho] = E_0 \ \& \ \mathcal{P}[\rho] = P_0(\sigma, z) \}, \quad (3.8)$$

which means that the equilibrium state is the density probability field ρ_{rsm} that satisfies the local normalization constraint (3.1), the energy constraint $\mathcal{E}[\rho] = E_0$ with \mathcal{E} given by (3.7), the incompressibility constraint $\mathcal{P}(\sigma, z)[\rho] = P_0(\sigma, z)$ with \mathcal{P} given by (3.4), and that maximizes the

entropy functional \mathcal{S} given by (3.3). We see that the parameters of this problem are the values of the constraints, which are prescribed by the initial condition $q_0(x, y, z)$.

3.2. Energy-ensrophy equilibrium states

3.2.1. Simplification of the variational problem

In practice, MRS equilibrium states are difficult to compute, because such computations involve the resolution of a variational problem with an infinite number of constraints. Computing the critical points of (3.8) is straightforward, see e.g. equation (A 1) of appendix A, but showing that second order variations of the entropy functional are negative is in general difficult. However, recent results have allowed considerable simplifications of the analytical computations of these equilibrium states (Bouchet 2008). The idea is first to prove equivalence (usually for a restricted range of parameters) between the complicated variational problem (3.8) and other variational problems more simple to handle, involving less constraints than the complicated problem, but characterized by the same critical points, and then to explicitly compute solutions of the simpler variational problem. The equivalence between the variational problems ensures that the solution of the simple problem are also solutions of the more complicated one. We will follow this approach in the following.

3.2.2. MRS equilibria characterized by linear $\bar{q} - \psi$ relations.

Starting from the MRS variational (3.8), it is shown in appendix A that any MRS equilibrium state characterized by a linear $\bar{q} - \psi$ relation is a solution of the variational problem

$$\mathcal{Z}_{cg}^{tot}(E_0, Z_0(z)) = \min_{\bar{q}} \{ \mathcal{Z}_{cg}^{tot}[\bar{q}] \mid \mathcal{E}[\bar{q}] = E_0 \} \quad (3.9)$$

with

$$\mathcal{Z}_{cg}^{tot}[\bar{q}] = \int_{-H}^0 dz \frac{\mathcal{Z}_{cg}}{Z_0}, \quad \mathcal{Z}_{cg} = \frac{1}{2} \int_{\mathcal{D}} dx dy \bar{q}^2, \quad (3.10)$$

where $Z_0(z)$ is the fine-grained enstrophy profile, E_0 the energy. This variational problem amounts to find the minimizer \bar{q}_m (a coarse grained PV field) of the coarse-grained enstrophy \mathcal{Z}_{cg}^{tot} (with $\mathcal{Z}_{cg}^{tot}[\bar{q}_m] = \mathcal{Z}_{cg}^{tot}(E_0, Z_0(z))$), among all the fields \bar{q} satisfying the constraint $\mathcal{E}[\bar{q}] = E_0$ given by (3.1).

Critical points of the variational problem (3.9) are computed by introducing a Lagrange multiplier β_l associated with the energy constraint, and by solving

$$\delta \mathcal{Z}_{cg}^{tot} + \beta_l \delta \mathcal{E} = 0,$$

where first variations of the functionals are taken with respect to the field \bar{q} . Because β_l is the Lagrange parameter associated with the energy constraint, it is called inverse temperature[†]. Using $\delta \mathcal{Z}_{cg}^{tot} = \int_{\mathcal{D}} dx dy \int_{-H}^0 dz \bar{q} \delta \bar{q} / Z_0$ and $\delta \mathcal{E} = - \int dx dy dz \psi \delta \bar{q}$, one finds that critical points of this problem are

$$\bar{q} = \beta_l Z_0 \psi. \quad (3.11)$$

The flow structure of these critical points can then be computed by solving

$$\Delta \psi + \frac{\partial}{\partial z} \frac{f_0^2}{N^2} \frac{\partial}{\partial z} \psi + \beta_l y = Z_0 \beta_l \psi \quad \text{with} \quad \partial_z \psi|_{z=0, z=-H} = 0. \quad (3.12)$$

Critical points can then be classified according to the value of their inverse temperature β_l . All

[†] The notation β is traditionally used in thermodynamics for inverse temperature. We use here the convention β_l for this inverse temperature, since $\beta = \partial_y f$ refers to the beta effect, i.e. to the variation of the Coriolis parameter with latitude.

the problem is then to find which of these critical point are actual minima of the coarse-grained enstrophy $\mathcal{Z}_{cg}^{tot}[\bar{q}]$ for a given energy $\mathcal{E}[\bar{q}] = E_0$.

MRS equilibrium states characterized by linear $\bar{q} - \psi$ relations are expected either in a low energy limit or in a strong mixing limit, see Bouchet & Venaille (2011) and references therein. Let us estimate when the low energy limit is valid. For a given distribution $P_0(\sigma, z)$ of PV levels σ , one can compute the maximum energy E_{max} among all the energies of the PV fields characterized by the distribution $P_0(\sigma, z)$. Low energy states characterized by the same distribution $P_0(\sigma, z)$ are therefore those characterized by $E \ll E_{max}$. The strong mixing limit, which can in some case overlap the low energy limit, is obtained by assuming $\beta_t \sigma \psi \ll 1$ in the expression (A 1) of the critical points of the MRS variational problem (3.8), see (Chavanis & Sommeria 1996).

3.2.3. Link with the phenomenological principle of enstrophy minimization and other equilibrium states

At a phenomenological level, the variational problem (3.9) can be interpreted as a generalization of the minimum enstrophy principle of Bretherton & Haidvogel (1976) to the continuous stratified flow: the equilibrium state minimize the vertical integral of the coarse-grained enstrophy normalized by the fine-grained enstrophy in each layer, with a global constraint given by energy conservation. This normalization is necessary to give a measure of the degree of mixing comparable from one depth z to another.

It has been shown by (Carnevale & Frederiksen 1987) that solutions of the minimum enstrophy problem of (Bretherton & Haidvogel 1976) for one layer quasi-geostrophic flows, are energy-enstrophy equilibrium states of the (Galerkin) truncated dynamics of these models, in the limit when the high-wave number cut-off goes to infinity. These energy-enstrophy equilibrium states were first introduced by in the framework of 2D truncated Euler flows by (Kraichnan 1967), then generalized by (Salmon *et al.* 1976) to one or few layers truncated quasi-geostrophic flows, and more recently generalized by Merryfield (1998) to truncated continuously stratified flows. Similar arguments than those of (Carnevale & Frederiksen 1987) would show that the minimum enstrophy problem (3.9) is equivalent to the variational problem considered by Merryfield (1998). We are therefore looking for the same class of equilibrium states. A first step toward the resolution of these variational problems have been achieved by Merryfield (1998), who computed critical points and discussed their vertical structure. In the next section, we built upon this work by relating explicitly the critical points to the constraints (Z_0, E) , and by selecting which of them are actual entropy maxima (or equivalently coarse-grained enstrophy minima), in different limit cases.

3.3. Enstrophy minima on a f -plane

In the previous subsection, we have shown that MRS equilibrium states characterized by a linear $\bar{q} - \psi$ relationship are solution of a minimum coarse-grained enstrophy variational problem (3.9). Such MRS equilibrium state will be referred to as ‘‘coarse-grained enstrophy minima’’ in the following. We found in the previous section that the affine relation of these coarse-grained enstrophy minima are of the form $\bar{q} = \beta_t Z_0 \psi$, with a coefficient proportional to the fine-grained enstrophy Z_0 , and are solutions of (3.12). The critical points of the variational problem (3.9) are any state \bar{q} satisfying these conditions. The aim of this subsection is to find which of these critical point \bar{q} are the actual coarse-grained enstrophy minima, solutions of variational problem (3.9), when there is no β -effect, but for arbitrary stratification N .

Injecting (3.11) in (3.10), and using the expression (3.7) with the constraint $E_0 = \mathcal{E}[\rho]$, one finds that the coarse-grained enstrophy of each critical point \bar{q} is given by

$$\mathcal{Z}_{cg}^{tot} = -\beta_t E_0 . \quad (3.13)$$

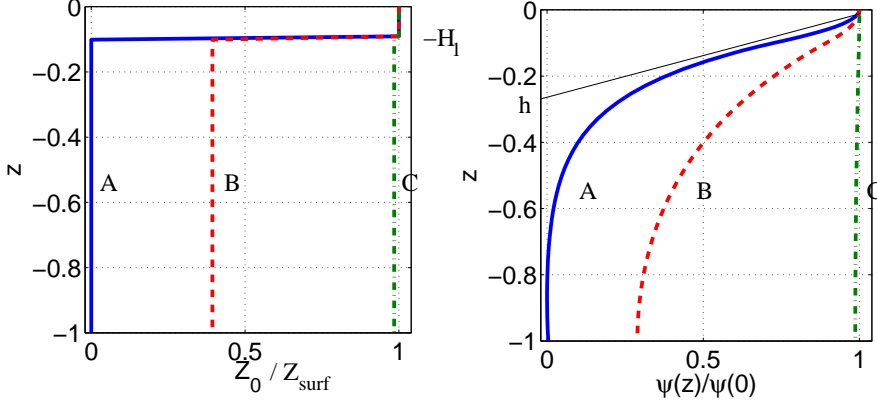


FIGURE 1. Left panel: three different fine grained enstrophy profiles. Right panel: corresponding vertical structure of statistical equilibrium states ($\psi(z)/\psi(0)$ on the left panel), in the case of constant stratification ($f_0^2/N^2 = 0.1$). The e -folding depth in case A is $h = f_0/NK$ (with here $K = 1$ for the statistical equilibrium state).

Remarkably, the coarse grained enstrophy of a critical point \bar{q} depends only on the inverse temperature β_t . We conclude that coarse-grained enstrophy minimum states are the solutions of (3.12) associated with the largest value β_t .

Projecting (3.12) on the Laplacian eigenmode $e_{l,k}(x,y)$ gives

$$\frac{\partial}{\partial z} \left(\frac{f_0^2}{N^2} \frac{\partial}{\partial z} \hat{\psi}_{k,l} \right) = (\beta_t Z_0 + K^2) \hat{\psi}_{k,l}, \quad (3.14)$$

with

$$\partial_z \hat{\psi}_{k,l}|_{z=0,-H} = 0, \quad K^2 = k^2 + l^2, \quad \psi = \sum_{k,l} \hat{\psi}_{k,l} e_{kl}.$$

We see that each critical point is characterized by a given wavenumber modulus K . Its vertical structure and the corresponding value of β_t must be computed numerically in the case of arbitrary profiles $Z_0(z)$. Let us consider the example shown in Fig. 1, for a two-step fine-grained enstrophy profile

$$Z_0 = Z_{\text{surf}} \Theta(z + H_1) + Z_{\text{int}} \Theta(-z - H_1), \quad H_1 \ll H, \quad (3.15)$$

where Θ is the Heaviside function, and for $Z_{\text{int}}/Z_{\text{surf}}$ varying between 0 and 1. We find that the minimum coarse-grained enstrophy states are always characterized by the gravest horizontal mode on the horizontal ($K = 1$). As for the vertical structure, we observe Fig. 1 a tendency toward more barotropic flows when the ratio $Z_{\text{int}}/Z_{\text{surf}}$ tends to one.

It is instructive to consider the limit cases $Z_{\text{surf}} = Z_{\text{int}}$ and $Z_{\text{int}} = 0$, corresponding respectively to case A and C of Fig. 1, for which minimum enstrophy can be explicitly solved. When the enstrophy profile is depth independent ($Z_0(z) = Z_{\text{int}}$, case C of figure 1), solutions of (3.14) are given by the modes $F_m(z) e_K(x,y)$ defined in subsection (2.2), and are associated with inverse temperatures $\beta_t = -(\lambda_m^2 + K^2)/Z_{\text{int}}$. We see that the maximum value of β_t is reached for the gravest horizontal mode ($K = 1$) and the gravest vertical mode ($\lambda_0 = 0$). It means that the coarse-grained enstrophy minimum state is barotropic.

When $Z_{\text{int}} = 0$ (case A of Fig. 1), it is straightforward to show that critical points, the solutions of (3.14), are SQG-like modes (see subsection 2.3) of e -folding depth $h = f_0/N(0)K$, associated with $\beta_t = -N(0)K/(H_1 Z_{\text{surf}} f_0)$ with corrections of order H_1/H and of order h/H . The coarse-

grained enstrophy minimum is therefore the SQG-like mode associated with $K = 1$ and with the largest e -folding depth $h = Lf/2\pi N$, where L is the domain length scale.

These examples show the importance of the conservation of fine-grained enstrophy to the vertical structure of the equilibrium state. The main result is that statistical mechanics predicts a tendency for the flow to reach the gravest Laplacian mode on the horizontal. The vertical structure associated with this state is fully prescribed by solving (3.14) with $K = 1$. Because the barotropic component of such flows are larger than solutions of (3.14) with $K > 1$, we can say that the inverse cascade on the horizontal is associated with a tendency to reach the gravest vertical mode compatible with the vertical fine-grained enstrophy profile Z_0 . This means a tendency toward barotropization, although in general, the fact that the profile Z_0 is non constant prevents complete barotropization.

3.4. Enstrophy minima on a β -plane

We now discuss how the results of the previous section generalize in presence of beta effect. For a given initial condition $\psi_0(x, y, z)$, increasing β increases the contribution of the (depth independent) available potential enstrophy defined as

$$Z_p = \beta^2 \int_{\mathcal{D}} dx dy y^2, \quad (3.16)$$

to the total fine-grained enstrophy profile $Z_0(z) = \int_{\mathcal{D}} dx dy q_0^2$, where q_0 is the initial PV field that can be computed by injecting ψ_0 in (2.2). For sufficiently large values of β , the PV field is dominated by the beta effect ($q_0 \approx \beta y$), Z_0 therefore tends to Z_p and becomes depth independent. Because statistical equilibria computed in the previous subsection were fully barotropic when the fine-grained enstrophy Z_0 was depth-independent, we expect a tendency toward barotropization by increasing β .

Consider for instance the case where ψ_0 is an SQG-like mode such that $q_0 = \beta y$ for $z < -H_1$, with $H_1 \ll H$ and associated with a surface fine-grained enstrophy $Z_0 = Z_{\text{surf}}$ for $z > -H_1$. The initial profile of fine-grained enstrophy Z_0 is thus given by (3.15), with the interior enstrophy $Z_{\text{int}} = Z_p$ prescribed by the available potential enstrophy (3.16). The question is then to determine whether the results obtained previously without beta effect still hold in presence of it.

We can actually compute the statistical equilibria in two limit cases. First, when $\beta = 0$, we recover the case with surface intensification of the fine grained enstrophy profile Z_0 , for which we found that statistical equilibria were the SQG-like modes associated with the gravest Laplacian horizontal modes, see subsection 3.3. Second, when β sufficiently large, such that $Z_p \gg Z_{\text{surf}}$, the statistical equilibria can be computed by considering the case of a constant fine-grained enstrophy profile Z_0 , which is the aim of the following paragraph.

To compute statistical equilibria in presence of beta effect and for a depth independent fine-grained enstrophy Z_0 , it is necessary to take into account the conservation of linear momentum (associated with translational invariance of the problem in the x direction), which provides an additional constraint $\mathcal{L}[\bar{q}] = L_0$, with

$$\mathcal{L}[\bar{q}] = \int_{\mathcal{D}} dx dy dz \bar{q} y. \quad (3.17)$$

(This constraint could have been taken into account in the cases without beta discussed in previous section, since the geometry of the flow was also translational invariant, but this would not have affected the results.) Critical points of the variational problem (3.9) with this additional constraint satisfy

$$\bar{q} = (\beta_t \psi - \mu y) Z_0, \quad (3.18)$$

where μ is the Lagrange multiplier associated with the linear momentum conservation. Equilib-

rium states therefore satisfy

$$Z_0 (\beta_t \psi - \mu y) = \Delta \psi + \frac{\partial}{\partial z} \left(\frac{f_0^2}{N^2} \frac{\partial}{\partial z} \psi \right) + \beta y. \quad (3.19)$$

The choice $\mu = -\beta/Z_0$ leads to the f -plane case: equilibrium states are then a linear combination of the gravest horizontal Laplacian eigenmodes ($K = 1$), with $\beta_t = -1/Z_0$.

Because a state characterized by $q = Z_0 (\beta_t \psi - \mu y)$ is stationary in a frame drifting in the zonal direction at speed $-\mu/\beta_t$, the equilibrium states associated with $\beta_t = -1/Z_0$ and $\mu = -\beta/Z_0$ and $K = 2\pi/L$ are drifting toward the west at speed of barotropic Rossby waves at the domain scale $U_{drift} = -4\pi^2\beta/L^2$.

Note that there could *a priori* exist local coarse-grained enstrophy minima for $\mu \neq \beta/Z_0$, but because such states involve other horizontal modes than the gravest ones, their enstrophy is necessary larger than states involving only the gravest Laplacian eigenmodes.

4. Numerical simulations

4.1. Experimental set-up

We consider in this section the final state organization of an initial SQG-like mode (defined in subsection 2.3), varying the values of β in a doubly periodic square domain of size $L = 2\pi$. More precisely, we consider a vertical discretization and an horizontal Galerkin truncation of the dynamics (2.1), for an initial potential vorticity field $q_0 = q_{0,surf}(x,y)\Theta(z+H_1) + \beta y$, such that $q_0 = \beta y$ in the interior ($-H < z < -H_1$) and $q_0 \approx q_{0,surf}$ in a surface layer $z > -H_1$. The surface PV $q_{surf}(x,y)$ is a random field with random phases in spectral space, and a Gaussian power spectrum peaked at wavenumber $K_0 = 5$, with variance $\delta K_0 = 2$, and normalized such that the total energy is equal to one ($E_0 = 1$). This corresponds to the case discussed subsection (3.4), with a vertical profile of fine-grained enstrophy given by (3.15), where the interior enstrophy is given by the available potential enstrophy (3.16): for $z < -H_1$, $Z_0 = 4\pi^4\beta^2/3$.

We perform simulations of the dynamics by considering a vertical discretization with 10 layers of equal depth, horizontal discretization of 512^2 , $H = 1$, and $F = (Lf_0/HN)^2 = 1$, using an energy and enstrophy conserving pseudo-spectral quasi-geostrophic model for the horizontal dynamics (Smith & Vallis 2001). We choose $H_1 = H/10$ for the initial condition, so that there is non zero enstrophy only in the upper layer in the absence of a beta effect. We also perform experiments in the presence of small scale dissipation (Laplacian viscosity or hyperviscosity), and found no qualitative differences as far as the large scale horizontal structure and the vertical structure of the flow were concerned. The only difference in presence of small scale dissipation is the decay of the enstrophy in each layer, because small scale dissipation smooths out PV filaments. Because of the energy cascade, the energy remains constant at lowest order even in presence of small scale dissipation.

Time integration of the freely evolving dynamics proceeds for about 250 eddy turnover times. Typically, i) the unstable initial condition leads to a strong turbulent stirring and the flow self-organizes rapidly into a few vortices, which takes a few eddy turnover times ii) same sign vortices eventually merge together on a longer time scale (a few dozens of eddy turnover time), and iii) the remaining dipole evolves very slowly on a slow time scale (more than hundreds of eddy turnover times). In absence of β -effect, a good indicator of the convergence is given by the convergence of the $q - \psi$ relation to a single functional relation. As we shall see in the following, this phenomenology is complicated by the presence of beta.

4.2. SQG-like dynamics ($\beta = 0$)

The case with $\beta = 0$ is presented on Fig. 2. The initial PV and streamfunction fields have horizontal structures around wave number $K_0 = 5$, which is associated with an SQG-like mode of typical e-folding depth $f_0/(NK_0) \approx 0.1$.

An inverse cascade in the horizontal leads to flow structures with an horizontal wavenumber K decreasing with time, associated with a tendency toward barotropization: the e -folding depth of the SQG-like mode increases as $f_0/2NK$. According to statistical mechanics arguments of the previous section, the flow should tend to the “gravest” horizontal SQG-like mode ($K = 1$), which is also the “gravest” vertical SQG mode, i.e. the one associated with the largest e -folding depth. The concomitant horizontal inverse cascade and the increase of the e -folding depth are observed on Fig. 2, showing good qualitative agreement between statistical mechanics and numerical simulations.

There are however quantitative differences between the observed final state organization and the prediction of energy-ensrophy statistical equilibria. Although the streamfunction is dominated by the gravest horizontal mode ($K = 1$), there remains “unmixed” blobs of potential vorticity in the cores of the final dipole. As seen on Fig. 3, the $\bar{q} - \psi$ relation is well defined (showing that the flow is in a stationary state), but it is not linear as predicted by energy-ensrophy theory. We observed that this relation does not change at all between 150 and 250 eddy turnover times, but its shape depends on the initial condition.

The presence of unmixed PV blobs in the final PV field implies the existence of structures smaller than wavenumber $K = 1$. Because each projection of the PV field on a different wavenumber is associated with an SQG-like mode associated with a different e -folding depth, the vertical structure of the flow is actually a linear combination of SQG-like modes associated with different wavenumbers. A consequence is that the effective e -folding depth of the kinetic energy is $f_0/(2NK^{\text{eff}})$. We estimated the coefficient $K_{\text{eff}} \approx 3.5$ by considering the linear $q - \psi$ relation passing through the extremal points of the observed $q - \psi$ relation of Fig. 3.

4.3. Effect of beta ($\beta \sim 1$)

We now consider the free evolution of the same initial condition $\psi_0(x, y, z)$ as in the previous subsection, but in presence of a beta plane. Because $\beta \neq 0$, the initial condition for potential vorticity is different than in the previous section: the total energy and initial velocity fields are the same as before, but the vertical profile of fine grained enstrophy is different, since there is now available potential enstrophy in the interior. As explained in subsection 3.3, this contribution from interior fine-grained enstrophy shall increase the relative barotropic component of the statistical equilibrium state. This is what is actually observed in the final state organization of Fig. 4. We conclude that in this regime, the beta effect is a catalyst[†] of barotropization, as predicted by statistical mechanics.

More surprisingly, the $q - \psi$ relation presented on Fig. 5 presents a very good agreement with the prediction of our computation of barotropic MRS equilibria carried in subsection 3.4: we observe a linear relation between $(q - \beta y)$ and ψ with a slope $\beta_t Z_0 = -1$. This means that the dipole structure observed in the streamfunction field is the actual gravest horizontal Laplacian eigenmode $K = 1$, and that this eigenmode is drifting westward at a speed β/K^2 .

4.4. Effect of strong Rossby waves ($\beta \gg 1$)

For large values of beta there is still an early stage, lasting a few eddy turnover times, of stirring of the unstable initial condition. But this initial stirring is limited to scales smaller than the Rhine’s

[†] By catalyst we do not mean a dynamical effect, as in chemistry, but simply the fact that barotropization in the final state is enhanced in presence of a beta plane.

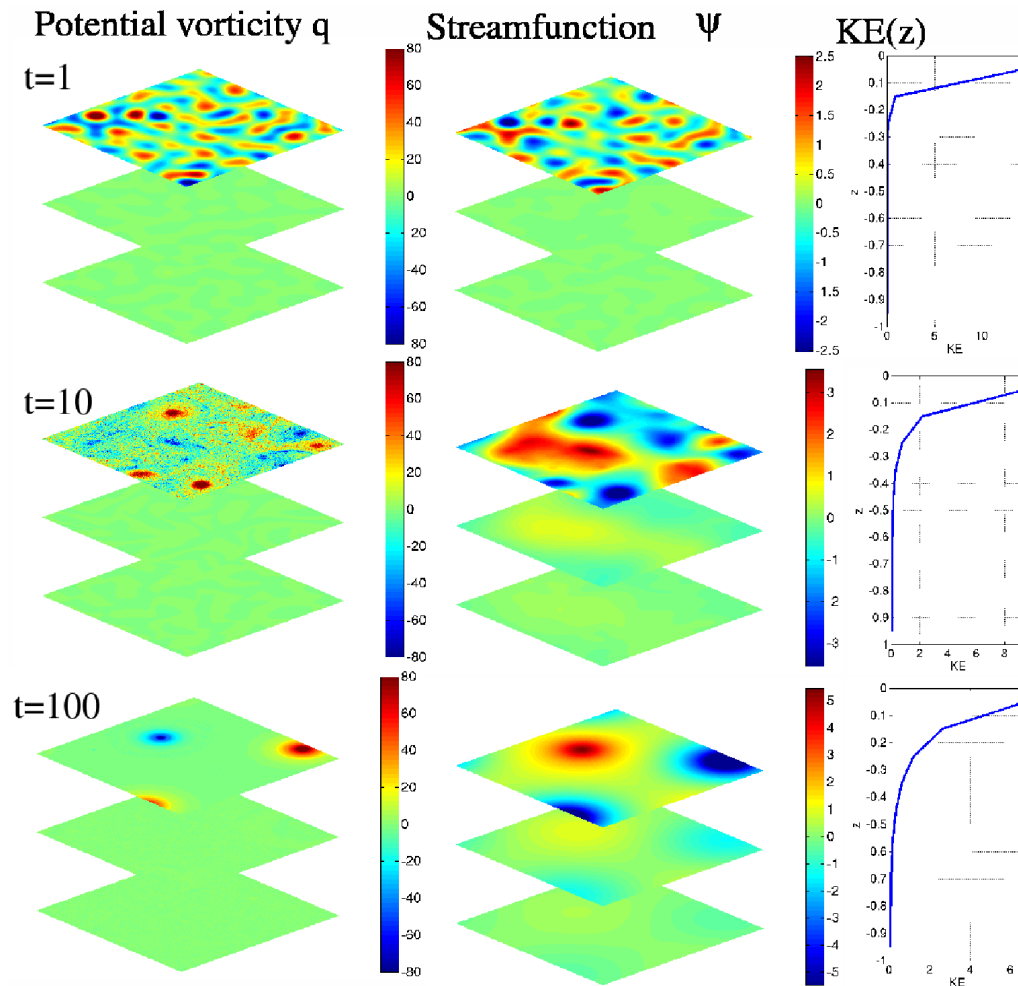


FIGURE 2. case $\beta = 0$ (SQG-like). Only the fields in upper, middle and lower layer are shown.

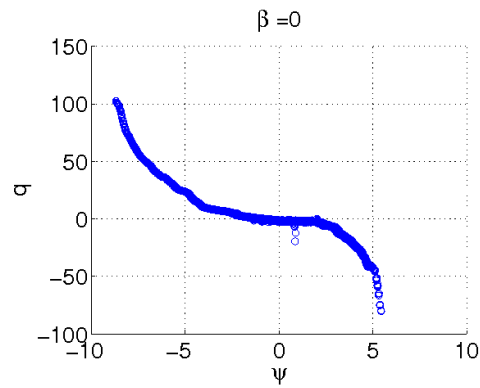


FIGURE 3. $q - \psi$ relation in the upper layer for $t = 250$ eddy turnover time.

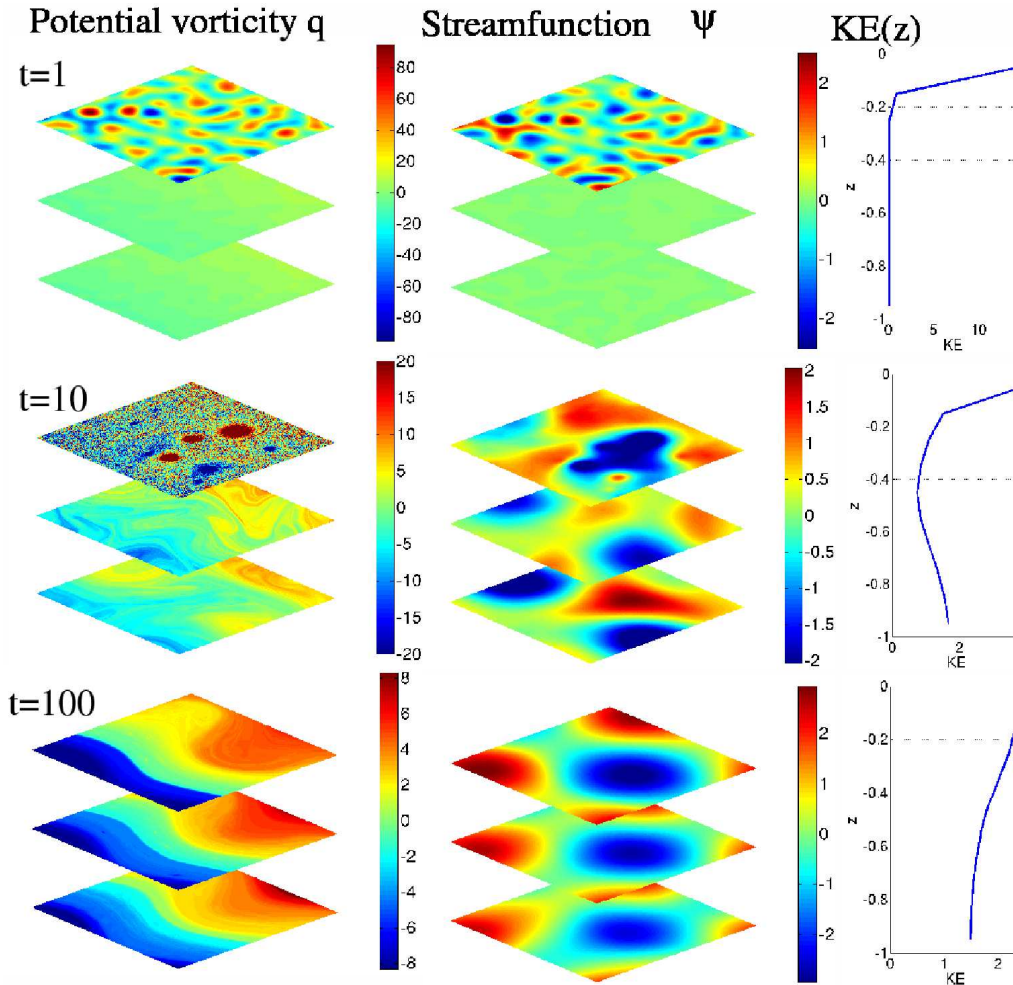


FIGURE 4. case $\beta = 2.1$. See Fig. 2 for legend. Note that the colors scales are changed at each time; this is why the interior “beta plane” is not visible in the upper panel of potential vorticity.

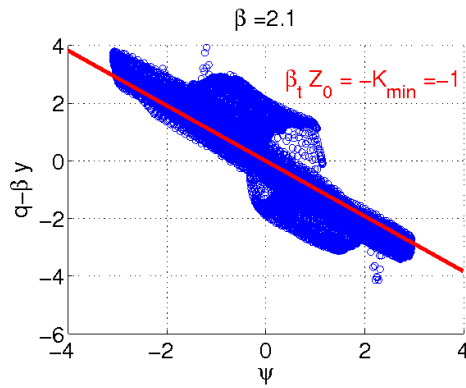
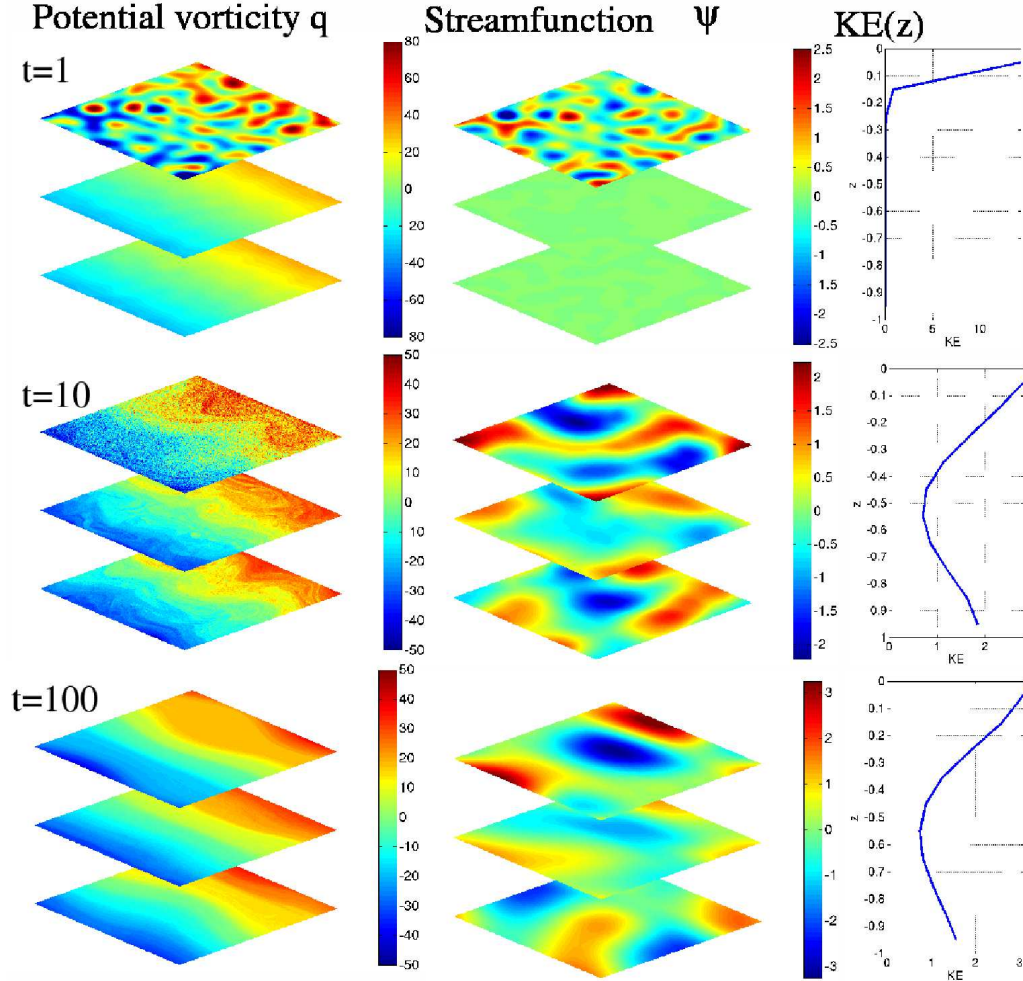


FIGURE 5. $q-\psi$ relation in the upper layer, at $t = 100$ eddy turnover time, for $\beta = 2.1$.

FIGURE 6. case $\beta = 10$, see Fig. 2 for legend.

scale[‡] $L_R = 2\pi E_0^{1/4} / \beta^{1/2}$, which eventually lead to a zonal PV field perturbed by Rossby waves around this scale, see Fig. 6. The dynamics is then dominated by Rossby waves, just as in one layer model Rhines (1977, 1975).

The PV and streamfunction fields in the final state clearly show that this vertical structure is imparted to Rossby waves superimposed to a stable mean flow (fig. 6).

Because the perturbation is confined in the upper layer, irreversible turbulent stirring occurs in the upper layer only, but not at the bottom. We did check that the global distribution of PV levels did not change in the lower layer through time, while this distribution was changed in the upper layer. In this case, the fundamental assumption that the system explores evenly the available phase space through turbulent stirring is not valid. One might reasonably argue that the statistical mechanic theory is incomplete, for it cannot identify the phase space that can be explored. In any case, we conclude that large values of beta prevent the convergence toward this equilibrium, leaving the question of the convergence itself to future work.

[‡] Here $E_0 = 1$ is the initial energy, so that $E_0^{1/2}$ is a good metric for typical velocities of the flow (assuming it becomes barotropic).

[t]

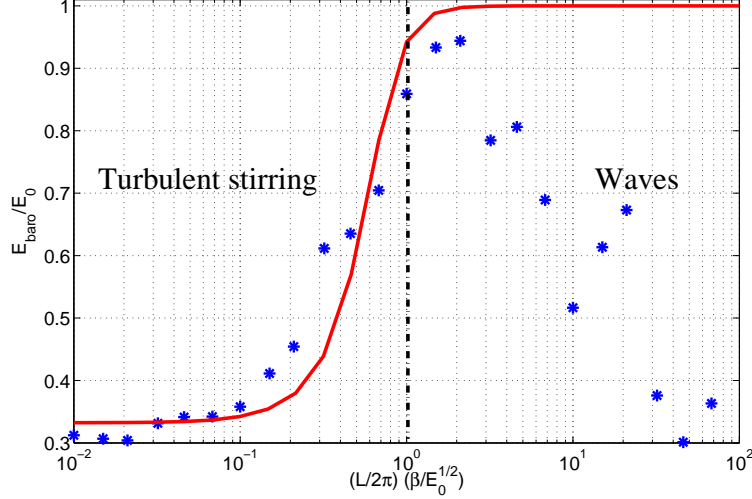


FIGURE 7. Variation of the Barotropic energy normalized by the total energy, varying $\beta E_0^{-1/2} L/2\pi$, at the end of each run, for the same initial condition ψ_0 ($L = 2\pi, E_0 = 1$). Red plain line: predictions from statistical mechanics (assuming $K_{\text{eff}} = 4$, see text), expected to be valid in a turbulent regime ($\beta E_0^{-1/2} L/2\pi < 1$). Magenta dashed line: curve $(\beta E_0^{-1/2} L/2\pi)^{-1/4}$, expected to be valid in a wave regime ($\beta E_0^{-1/2} L/2\pi > 1$).

4.5. Turbulent stirring vs wave dynamics

We summarize the effect of planetary vorticity gradients on Fig. 7 by considering the ratio E_{baro}/E_0 of barotropic energy to total energy, after 250 eddy turnover-time, for varying values of β . The plain red line represents statistical mechanics predictions. In order to allow comparison with the numerical experiments, for which the horizontal PV field did present structures smaller than the gravest mode $K = 1$ for low values of β (see subsection 4.2), we computed the vertical structure with equation (3.14), using $K_{\text{eff}} = 3.5$, and using the enstrophy profile $Z_0(\beta)$ of the initial condition ψ_0 . Strictly speaking, this effective horizontal wavenumber K_{eff} should vary with beta between $K_{\text{eff}} = 3.5$ for $\beta = 0$ and $K_{\text{eff}} = 1$ for $\beta > 1$, but taking into account this variations would not change much the shape of the red plain curve.

The critical value of β between the turbulent regime for which statistical mechanics prediction are useful and the wave regime can be estimated by considering the case in which the Rhines scale $L_{Rh} \sim 2\pi \left(E_0^{1/2} / \beta \right)^{1/2}$ is of the order of the domain scale $L = 2\pi$. Here the total energy is $E_0 = 1$, which renders the critical value $\beta \sim 1$ in our simulations.

Because the ratio E_{baro}/E_0 gives incomplete information on the flow structure, and because dynamical information is useful to understand where statistical mechanics fails to predict the vertical structure, we represent on Fig. 8 the temporal evolution of the energies E_m of the baroclinic modes[†] defined in (2.5).

For small values of beta (see the first panel of Fig. 8), the dynamics reaches the equilibrium after a turbulent stirring during few eddy turnover times, and the contribution of each mode E_m simply reflects the SQG-like structure of the final state. For values of beta of order one (see the second panel of Fig. 8), the same turbulent stirring mechanism leads to a barotropic flow after a

[†] Note that with this notation, $E_{m=0} = E_{\text{baro}}$ is the energy of the barotropic mode, which is in general different from the total energy of the initial condition E_0 .

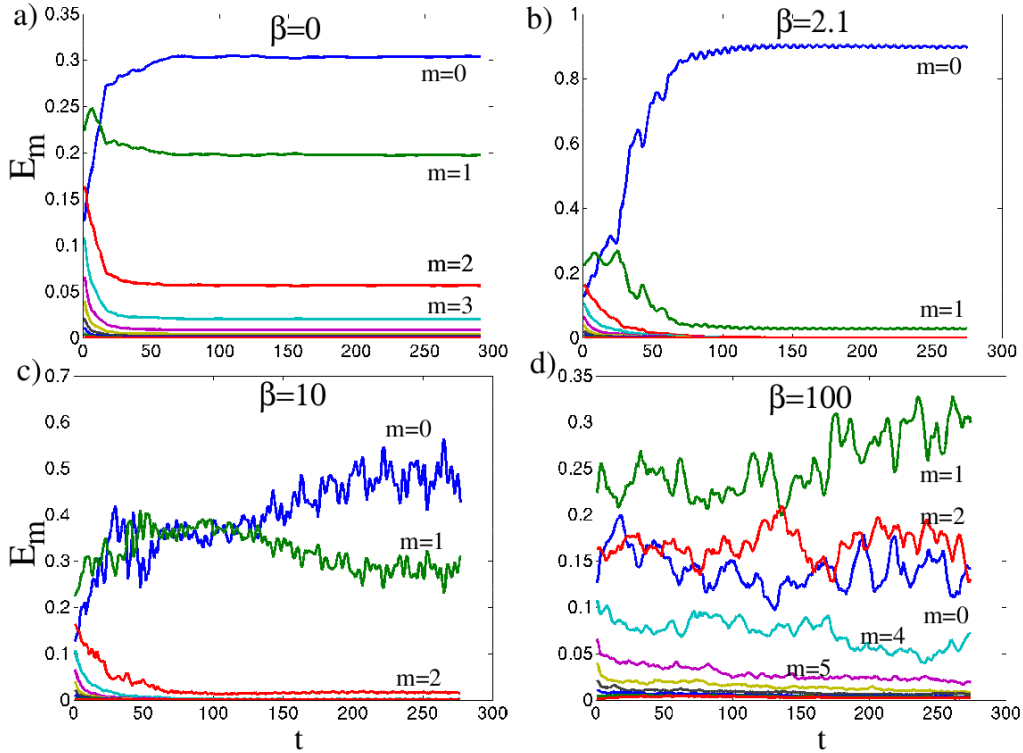


FIGURE 8. Temporal evolution of the contribution of the energy of each baroclinic mode to the total energy, for different values of β . The modes are indexed by m , with $m = 0$ the barotropic mode and $m = 1$ the first baroclinic mode.

few eddy turnover times. For values of β larger than one, there is still an initial turbulent stirring regime, but the duration of this regime tend to diminish with larger values of beta. We observe a slow transfer of energy from first baroclinic to the barotropic mode in the case $\beta = 10$ (see the third panel of Fig. 8), but it is unclear if it will eventually lead to a condensation of the energy in the barotropic mode. In the case $\beta = 100$ (see the fourth panel of Fig. 8), there is in average almost no energy transfers between the vertical modes, after the initial stirring regime. Again, it is unclear if interactions between waves would eventually condense their energy into the barotropic mode in a longer numerical run. The strong temporal fluctuations of the contribution of each vertical mode visible on the wave regime of figure Fig. 8 may explain why they are large variations of $E_{\text{baro}}/E_{\text{tot}}$ (in addition to the mean tendency of a decay with β) in the wave regime of figure 7.

5. Discussions and conclusion

We have used statistical mechanics to try to predict the flow structure resulting from the self-organization of freely evolving inviscid stratified quasi-geostrophic flows. The only assumption of the theory is that the flow explores evenly the available phase space. In order to compute explicitly statistical equilibria, and to discuss basic physical properties of these equilibria, we have focused on MRS equilibria characterized by linear relation between potential vorticity and streamfunction. For such MRS equilibrium states, one only need to know the total energy and the enstrophy in each layer, although all the invariants are implicitly taken into account.

We explained that these states are expected in a low energy limit or in a strong mixing limit, and that they are also the equilibria of the truncated quasi-geostrophic flows in the limit of infinite wave number cutoff (the so called “energy-ensrophy” equilibria). By applying a method proposed by (Bouchet 2008), we have shown that MRS equilibria characterized by a linear $q - \psi$ relation are solutions of a minimum coarse-grained enstrophy variational problem, which generalizes the Bretherton-Haidvogel minimum enstrophy principle to the stratified case.

The central result of the paper is to have elucidated the physical consequences of the conservation of the fine-grained enstrophy $Z_0(z)$ on the structure of the equilibrium states. We showed first that the affine coefficients between the coarse-grained PV field and the streamfunction are proportional to the fine-grained enstrophy: $\bar{q} = \beta_1 Z_0(z) \psi$. This relation allowed to compute explicitly the statistical equilibria, and to discuss their structure depending on the profile $Z_0(z)$. When this profile Z_0 is depth independent, the equilibrium state is fully barotropic, whatever the stratification profile N . When this profile Z_0 is surface intensified, the equilibrium state is an SQG-like mode, characterized by an e -folding depth $\sim f_0/NK$, where $1/K$ is bounded by the domain scale. Since the e -folding depth increases with K^{-1} , larger horizontal flow structures imply “more barotropic” flows. Since statistical equilibria are associated with the gravest Laplacian horizontal modes ($K = 1$), the equilibrium state is the “most barotropic one” given an enstrophy profile Z_0 .

We conclude that the dynamics leads to the *gravest horizontal mode on the horizontal (inverse cascade), associated with the gravest vertical structure consistent with the conservation of the fine grained enstrophy. The flow becomes fully barotropic when the fine-grained enstrophy profile is depth independent.*

These results can be used to understand the role of beta effect in barotropization process in the following way: consider an initial SQG-like flow, with $\beta = 0$, prescribed by its streamfunction; its enstrophy profile is surface intensified, and so will be the equilibrium state. But when one switches on the beta effect, with the same initial streamfunction, the contribution of the depth independent part of the fine-grained enstrophy increases, which means a tendency toward a more barotropic equilibria, according to the previous conclusion. This simply reflects the fact that in physical space, the initial SQG-like mode stirs the interior PV field (initially a beta plane), which in turn induces an interior flow, which stirs even more the interior PV field, and so on.

On the one hand, when the beta effect becomes large enough, the PV distribution at each depth z becomes prescribed by the initial beta plane, so the most probable state should be also characterized by a depth independent PV field, i.e. by a barotropic flow.

On the other hand, to reach the equilibrium state, the PV field must be stirred enough to explore the phase space. Yet large values of beta stabilize the initial condition, the system is trapped in a stable state different from the equilibrium state, and the flow dynamics becomes dominated by the interaction between Rossby waves rather than by turbulent stirring. The reason of this trapping is that the dynamics can not provide by itself sufficient perturbations to escape from the stable state and to explore other regions of the phase space, which would attract the system toward the equilibrium state. We observed in numerical simulations that this wave regime did not lead to a barotropization of the flow after a few hundred turnover times. We do not know if still longer numerical runs would lead to more barotropization. We estimated the critical value of beta between the turbulent stirring regime and the Rossby wave regime as the value such that The Rhines scale is of the order of the domain scale, which gives $\beta = 4\pi^2 E_0^{1/2} / L^2$.

We now discuss how these results may apply to the mesoscale ocean, and in what respect they may provide interesting eddy parametrization. First, we have considered the relaxation of an initial condition by an inviscid flow. Real oceanic flows are forced dissipated. Statistical mechanics predictions should apply if a typical time scale for self-organization is smaller than typical time scale of forcing and dissipation. This issues of forcing and dissipation leads to another difficulty:

what is the domain in which the flow self-organizes ? Strictly speaking, it should be the oceanic basin. But forcing and dissipation become dominant at basin scale (with, for instance, the Sverdrup balance setting the gyre structures). In practice, on a phenomenological basis, one could still apply the statistical mechanics predictions by considering an artificial domain scale with prescribed a scale of arrest for the inverse cascade, governed say by dissipation processes, but which could not be predicted by statistical mechanics itself.

We have also neglected bottom friction, because equilibrium statistical mechanics apply for non-dissipative systems. It is generally believed that bottom friction plays a key role in the vertical structure of oceanic flows Arbic & Flierl (2004); Thompson & Young (2006); Venaille *et al.* (2011). On a phenomenological basis, quasi-statistical equilibria could be computed in the high bottom friction limit by adding a constraint of zero velocity at the bottom, for instance by considering $\psi(-H) = 0$ in equation (3.14).

Third, equilibrium statistical mechanics predict the final state organization of the freely evolving inviscid dynamics, but neither predicts the route toward this state nor the corresponding typical time scales for the convergence toward this state. Various parametrizations that relax the flow toward the equilibrium state, following a path of maximum entropy production have been proposed, see Kazantsev *et al.* (1998); Robert & Sommeria (1992). These parametrization satisfy basic physical constraints satisfied by the dynamics (PV distribution conservation and energy conservation), but the actual dynamics may in some cases follow a different path than one of maximum entropy production.

The results presented in this paper have highlighted the important role of the fine-grained enstrophy profile, for this imposes strong constraints for the eddy structures. On a practical point of view, from the perspective of eddy parameterizations, our result suggest that rather than assuming a vertical structure of eddies given by SQG modes, or given by combination of barotropic and first baroclinic modes, one could compute the eddy structure with equation (3.14), assuming that K is the scale of arrest, and Z_0 an enstrophy profile that could be deduced from the resolved flow. For instance, Z_0 could be set by the structure of the most unstable mode of local baroclinic instabilities.

Acknowledgments This work was supported by DoE grant de-sc0005189 and NOAA grant NA08OAR4320752. AV warmly thank F. Bouchet and J. Sommeria for fruitful discussions, and K.S. Smith for sharing his QG code.

Appendix A. Minimum enstrophy states

The aim of this appendix is to show that the class of MRS statistical associated with a linear $\bar{q} - \psi$ relation can be computed by solving a minimum enstrophy variational problem satisfied by the coarse-grained state \bar{q} . This is a direct consequence of a more general result of Bouchet (2008), see also Naso *et al.* (2010).

A.1. Variational problem of the MRS statistical theory

We consider the variational problem (3.8) given by MRS theory. To compute its critical points, we introduce the Lagrange multipliers $\beta_r, \alpha(\sigma, z), \zeta(x, y)$ associated respectively with the energy \mathcal{E} (3.7), with the global PV distribution \mathcal{P} (3.4), and with the local normalization constraint \mathcal{N} given by (3.1). Critical points are solutions of

$$\delta \mathcal{S} - \beta_r \delta \mathcal{E} - \left(\int_{-H}^0 dz \int_{\Sigma} d\sigma \alpha \delta \mathcal{P} \right) - \left(\int_D dx dy \zeta \delta \mathcal{N} \right) = 0,$$

where first variations are taken with respect to the field ρ . This equation and the normalization constraint lead to

$$\rho = \frac{1}{z_\alpha(\beta_t \psi)} \exp(\beta_t \psi \sigma - \alpha(\sigma, z)), \text{ with } z_\alpha(u) = \int_\Sigma d\sigma \exp(u\sigma - \alpha(\sigma, z)). \quad (\text{A } 1)$$

The coarse-grained potential vorticity field associated with this state is

$$\bar{q} = \int_\Sigma d\sigma \sigma \rho = f_\alpha(\beta_t \psi), \text{ with } f_\alpha(u) = \frac{d}{du} \ln z_\alpha; \quad (\text{A } 2)$$

and the local fluctuations of potential vorticity are

$$\overline{q^2} - \bar{q}^2 = \int_\Sigma d\sigma \sigma^2 \rho = f'_\alpha(\beta_t \psi), \quad (\text{A } 3)$$

where f'_α is the derivative of f_α .

A.2. Case of a linear $q - \psi$ relation

Here we focus on a particular class of solutions, assuming

$$f_\alpha(u) = \Omega(z)u,$$

where the coefficient $\Omega(z)$ will be expressed in term of the constraints of the problem. Equations (A 2) and (A 3) give the $q - \psi$ relation and the fluctuations

$$\bar{q} = \beta_t \Omega(z) \psi, \quad \Omega = \overline{q^2} - \bar{q}^2.$$

Integrating the fluctuations on the horizontal leads to

$$\Omega = \int_{\mathcal{D}} dx dy (\overline{q^2} - \bar{q}^2) = 2(\mathcal{E} - \mathcal{E}_{cg}), \text{ with} \quad (\text{A } 4)$$

$$\mathcal{E}[\rho] = \frac{1}{2} \int_{\mathcal{D}} dx dy \left(\int_\Sigma d\sigma \sigma^2 \rho \right), \quad \mathcal{E}_{cg}[\rho] = \frac{1}{2} \int_{\mathcal{D}} dx dy \left(\int_\Sigma d\sigma \sigma \rho \right)^2.$$

Using the relations (A 1-A 2), we find that

$$z_\alpha(u) = (2\pi\Omega)^{1/2} \exp\left(\frac{1}{2}\Omega u^2\right), \quad \rho = \frac{1}{(2\pi\Omega)^{1/2}} \exp\left(-\frac{(\sigma - \bar{q})^2}{2\Omega}\right), \quad \alpha(\sigma, z) = \frac{\sigma^2}{2\Omega}. \quad (\text{A } 5)$$

A.3. Link with a minimum enstrophy problem

Solution of dual, less constrained variational problem is always a solution of the more constrained problem for some values of the constraints (Ellis *et al.* 2000). We relax the constraints on the PV distribution by introducing the Legendre Transform \mathcal{G}_α of the entropy associated with this constraint, taking into account the conservation of the total energy E_0 and of the fine-grained enstrophy $Z_0(z)$ in each layer:

$$G(E_0, Z_0(z), \alpha) = \min_{\rho, \mathcal{N}[\rho]=1} \{ \mathcal{G}_\alpha[\rho] \mid \mathcal{E}[\rho] = E_0, \mathcal{Z}[\rho] = Z_0(z) \}, \quad (\text{A } 6)$$

$$\mathcal{G}_\alpha = \int_{\mathcal{D}} dx dy \int_{-H}^0 dz \int d\sigma \rho \ln \rho + \int_{-H}^0 dz \int_\Sigma d\sigma \alpha \int_{\mathcal{D}} dx dy \rho, \quad (\text{A } 7)$$

where \mathcal{E} is given by (3.7), where the pdf field is locally normalized using (3.1). Equations (A 5) and (A 4) give

$$\alpha(\sigma, z) = \frac{\sigma^2}{4(Z_0 - \mathcal{Z}_{cg})} \quad \text{and} \quad \rho = \frac{\exp\left(-\frac{(\sigma - \bar{q})^2}{4(Z_0 - \mathcal{Z}_{cg})}\right)}{(4\pi(Z_0 - \mathcal{Z}_{cg}))^{1/2}}$$

Injecting these expressions into (A 7) yields

$$\mathcal{G}_\alpha[\rho] = \frac{1}{2} \int_{-H}^0 dz w\left(\frac{\mathcal{Z}_{cg}}{Z_0}\right) + cst, \quad \text{with} \quad w(x) = -\ln(1-x) + \frac{1}{1-x}$$

In the limit $x \ll 1$, we have $w(x) \approx x$, so finding the minimizer ρ_m of \mathcal{G}_α with the (global) constraint on the energy and the enstrophy is equivalent of finding the minimizer of the functional $\int_{-H}^0 dz \mathcal{Z}_{cg}[\bar{q}]/Z_0$ with the same constraints. The hypothesis that $\mathcal{Z}_{cg} \ll Z_0$ is consistent with the “strong mixing limit” ($\beta_t \psi \sigma \ll 1$) or the low energy limit for which MRS equilibria are characterized by a linear relation between potential vorticity and streamfunction. We conclude that MRS equilibrium states characterized by a linear $\bar{q} - \psi$ relation are solutions of the variational problem (3.9).

REFERENCES

- ARBIC, B. K. & FLIERL, G. R. 2004 Baroclinically Unstable Geostrophic Turbulence in the Limits of Strong and Weak Bottom Ekman Friction: Application to Midocean Eddies. *Journal of Physical Oceanography* **34**, 2257.
- BOUCHET, F. 2008 Simpler variational problems for statistical equilibria of the 2d euler equation and other systems with long range interactions. *Physica D Nonlinear Phenomena* **237**, 1976–1981.
- BOUCHET, F. & CORVELLEC, M. 2010 Invariant measures of the 2D Euler and Vlasov equations. *Journal of Statistical Mechanics: Theory and Experiment* **8**, 21.
- BOUCHET, F. & SOMMERIA, J. 2002 Emergence of intense jets and Jupiter’s Great Red Spot as maximum-entropy structures. *Journal of Fluid Mechanics* **464**, 165–207.
- BOUCHET, F. & VENAILLE, A. 2011 Statistical mechanics of two dimensional and geophysical turbulent flows. *accepted for Physics Reports*.
- BRETHERTON, F.P. 1966 Critical layer instability in baroclinic flows. *Quart. J. Roy. Meteor. Soc.* **92**, 325–334.
- BRETHERTON, F. P. & HAIDVOGEL, D. B. 1976 Two-dimensional turbulence above topography. *Journal of Fluid Mechanics* **78**, 129–154.
- CARNEVALE, G. F. & FREDERIKSEN, J. S. 1987 Nonlinear stability and statistical mechanics of flow over topography. *Journal of Fluid Mechanics* **175**, 157–181.
- CHARNEY, J. G. 1971 Geostrophic Turbulence. *Journal of Atmospheric Sciences* **28**, 1087–1094.
- CHAVANIS, P. H. & SOMMERIA, J. 1996 Classification of self-organized vortices in two-dimensional turbulence: the case of a bounded domain. *J. Fluid Mech.* **314**, 267–297.
- ELLIS, R. S., HAVEN, K. & TURKINGTON, B. 2000 Large deviation principles and complete equivalence and nonequivalence results for pure and mixed ensembles. *Journal of Statistical Physics* **101**, 999–1064.
- KAZANTSEV, E., SOMMERIA, J. & VERRON, J. 1998 Subgrid-Scale Eddy Parameterization by Statistical Mechanics in a Barotropic Ocean Model. *Journal of Physical Oceanography* **28**, 1017–1042.
- KRAICHNAN, R. H. 1967 Inertial Ranges in Two-Dimensional Turbulence. *Physics of Fluids* **10**, 1417–1423.
- KRAICHNAN, R. H. & MONTGOMERY, D. 1980 Two-dimensional turbulence. *Reports on Progress in Physics* **43**, 547–619.
- LAPEYRE, G. 2009 What Vertical Mode Does the Altimeter Reflect? On the Decomposition in Baroclinic Modes and on a Surface-Trapped Mode. *Journal of Physical Oceanography* **39**, 2857.
- LAPEYRE, G. & KLEIN, P. 2006 Dynamics of the upper oceanic layers in terms of surface quasigeostrophy theory. *Journal of Physical Oceanography* **36**, 165–176.
- MCWILLIAMS, J. C., WEISS, J. B. & YAVNEH, I. 1994 Anisotropy and Coherent Vortex Structures in Planetary Turbulence. *Science* **264**, 410–413.

- MERRYFIELD, W. J. 1998 Effects of stratification on quasi-geostrophic inviscid equilibria. *Journal of Fluid Mechanics* **354**, 345–356.
- MICHEL, J. & ROBERT, R. 1994 Large deviations for young measures and statistical mechanics of infinite dimensional dynamical systems with conservation law. *Communications in Mathematical Physics* **159**, 195–215.
- MILLER, JONATHAN 1990 Statistical mechanics of euler equations in two dimensions. *Phys. Rev. Lett.* **65** (17), 2137–2140.
- NASO, A., CHAVANIS, P. H. & DUBRULLE, B. 2010 Statistical mechanics of two-dimensional Euler flows and minimum enstrophy states. *European Physical Journal B* **77**, 187–212.
- RHINES, P., ed. 1977 *The dynamics of unsteady currents*, , vol. 6. Wiley and Sons.
- RHINES, P. B. 1975 Waves and turbulence on a β -plane. *J. Fluid. Mech.* **69**, 417–443.
- ROBERT, R. 1990 Etats d'équilibre statistique pour l'écoulement bidimensionnel d'un fluide parfait. *C. R. Acad. Sci.* **1**, 311:575–578.
- ROBERT, R. & SOMMERIA, J. 1991 Statistical equilibrium states for two-dimensional flows. *J. Fluid Mech.* **229**, 291–310.
- ROBERT, R. & SOMMERIA, J. 1992 Relaxation towards a statistical equilibrium state in two-dimensional perfect fluid dynamics. *Physical Review Letters* **69**, 2776–2779.
- SALMON, R. 1998 *Lectures on Geophysical Fluid Dynamics*. Oxford University Press.
- SALMON, R., HOLLOWAY, G. & HENDERSHOTT, M. C. 1976 The equilibrium statistical mechanics of simple quasi-geostrophic models. *Journal of Fluid Mechanics* **75**, 691–703.
- SCHECTER, D. A. 2003 Maximum entropy theory and the rapid relaxation of three-dimensional quasi-geostrophic turbulence. *Physical Review E* **68** (6), 066309.
- SCOTT, R. B. & WANG, F. 2005 Direct Evidence of an Oceanic Inverse Kinetic Energy Cascade from Satellite Altimetry. *Journal of Physical Oceanography* **35**, 1650.
- SMITH, K. S. & VALLIS, G. K. 2001 The Scales and Equilibration of Midocean Eddies: Freely Evolving Flow. *Journal of Physical Oceanography* **31**, 554–571.
- THOMPSON, A. F. & YOUNG, W. R. 2006 Scaling Baroclinic Eddy Fluxes: Vortices and Energy Balance. *Journal of Physical Oceanography* **36**, 720.
- VALLIS, G. K. 2006 *Atmospheric and Oceanic Fluid Dynamics*.
- VENAILLE, A. & BOUCHET, F. 2011 Oceanic rings and jets as statistical equilibrium states. *Journal of Physical Oceanography* **41** (10), 1860–1873.
- VENAILLE, A., VALLIS, G.K. & SMITH, K.S. 2011 Baroclinic turbulence in the ocean: analysis with primitive equation and quasi-geostrophic simulations. *Journal of Physical Oceanography* **41** (9), 1605–1623.